HHS Public Access

Author manuscript

Adv Healthc Mater. Author manuscript; available in PMC 2022 February 13.

Published in final edited form as:

Adv Healthc Mater. 2017 August ; 6(16): . doi:10.1002/adhm.201700523.

Dual Cross-Linked Biofunctional and Self-Healing Networks to Generate User-Defined Modular Gradient Hydrogel Constructs

Zhao Wei Dr.,

Department of Chemical and Biomolecular Engineering, The Institute for NanoBioTechnology, Physical-Sciences Oncology Center, Johns Hopkins University, Baltimore, MD 21218, USA

Daniel M. Lewis,

Department of Chemical and Biomolecular Engineering, The Institute for NanoBioTechnology, Physical-Sciences Oncology Center, Johns Hopkins University, Baltimore, MD 21218, USA

Yu Xu,

Department of Chemical and Biomolecular Engineering, The Institute for NanoBioTechnology, Physical-Sciences Oncology Center, Johns Hopkins University, Baltimore, MD 21218, USA

Prof. Sharon Gerecht*

Department of Chemical and Biomolecular Engineering, The Institute for NanoBioTechnology, Physical-Sciences Oncology Center, Johns Hopkins University, Baltimore, MD 21218, USA; Department of Materials Science and Engineering, Johns Hopkins University, Baltimore, MD 21218, USA

Abstract

Gradient hydrogels have been developed to mimic the spatiotemporal differences of multiple gradient cues in tissues. Current approaches used to generate such hydrogels are restricted to a single gradient shape and distribution. Here, a hydrogel is designed that includes two chemical cross-linking networks, biofunctional, and self-healing networks, enabling the customizable formation of modular gradient hydrogel construct with various gradient distributions and flexible shapes. The biofunctional networks are formed via Michael addition between the acrylates of oxidized acrylated hyaluronic acid (OAHA) and the dithiol of matrix metalloproteinase (MMP)-sensitive cross-linker and RGD peptides. The self-healing networks are formed via dynamic Schiff base reaction between *N*-carboxyethyl chitosan (CEC) and OAHA, which drives the modular gradient units to self-heal into an integral modular gradient hydrogel. The CEC-OAHA-MMP hydrogel exhibits excellent flowability at 37 °C under shear stress, enabling its injection to generate gradient distributions and shapes. Furthermore, encapsulated sarcoma cells respond to the gradient cues of RGD peptides and MMP-sensitive cross-linkers in the hydrogel. With these superior properties, the dual cross-linked CEC-OAHA-MMP hydrogel holds significant potential for generating customizable gradient hydrogel constructs, to study and guide cellular

* gerecht@jhu.edu .

Supporting Information

Supporting Information is available from the Wiley Online Library or from the author.

Conflict of Interest

The authors declare no conflict of interest.

responses to their microenvironment such as in tumor mimicking, tissue engineering, and stem cell differentiation and morphogenesis.

Keywords

biofunctional networks; dual cross-links; modular gradient hydrogels; self-healing properties

Cells experience a multitude of signals in the extracellular matrix (ECM) in vivo, which include spatiotemporal gradients of multiple chemical and physical cues such as matrix stiffness,[1,2] oxygen tension,[3] glucose concentration,[4,5] and various other biological molecules (cytokines, growth factors, adhesive ligands, etc.).[6–8] These spatial and temporal gradients in the microenvironment play important roles in regulating various cellular behaviors and functions including spreading, proliferation, migration, differentiation, and morphogenesis.[9–12] Indeed, a key goal of tissue engineering is the development of 3D scaffolds by incorporating different physiologically relevant gradients that replicate the complexity of native tissues and organs.[13–15]

Due to their ECM-like structures, viscoelasticity and diffusivity, polymeric hydrogels have been utilized to recapitulate many aspects of cellular microenvironments in mimicry scaffolds for tissue engineering or therapeutics.[16–19] However, recapitulating gradients in polymeric hydrogels is challenging due to the unrestrained polymerization process that typically results in uniformly distributed networks. To overcome this limitation, various techniques, including microfluidics, photolithography, thermal cross-linking, and micropatterning, have been widely applied to generate hydrogels with different gradients.[20–23] For example, by using microfluidic techniques, He et al. generated a gradient of the cell-adhesive ligand, the RGD peptide (Arg-Gly-Asp-Ser), in a poly(ethylene glycol) (PEG) hydrogel by pumping a high concentration of RGD into a microchannel embedded with a lower RGD concentration.[24] Other studies have created elastic modulus gradients in PEG-diacrylate hydrogels using pressures from 2.5 to 10 kPa via the grayscale mask cross-linking approach.[25] However, current strategies for generating gradient hydrogels are restricted to a single gradient shape and distribution, which impedes their potential use in tissue engineering to recapitulate the complex structural and cellular characteristics of in vivo environments.[8,13] Therefore, material synthesis must be improved to create gradient hydrogel systems with advanced components, including a more flexible shape and a customizable gradient design, all of which has been challenging.

Here, we report modular gradient hydrogel constructs generated by exploiting self-healing hydrogel units, which can autonomously restore the integrity of their network structures and functionalities after damage without an external stimulus.[26,27] A series of tiny self-healing hydrogel units that contain cues at various concentrations are arranged by a user-defined sequence, leading to an integral hydrogel construct with gradient distributions. Moreover, the self-healing hydrogels are flowable under shear stress, allowing their injection and the injected fragments could rapidly re-solidify after cessation of the extruded stress.[28,29] In this study, we loaded the tiny modular self-healing hydrogel units into a syringe in a user-defined sequence. We hypothesized that, following injection, the sequentially squeezed

hydrogel fragments would self-heal into a bulk and integral hydrogel constructs with a gradient distribution as defined during hydrogel loading. The shape of the injected modular gradient hydrogel construct could be freely varied depending on the “writing route” of the syringe. Therefore, using this new injectable/self-healing approach, we can easily achieve both control over the hydrogel construct shape and gradient distribution, which has not been previously explored.

We designed a dual cross-linked polysaccharide-based hydrogel network with both biofunctionality and self-healing properties (Figure 1a). The polysaccharide portion is made of chitosan and hyaluronic acid, which were chosen as the backbone of the polymer network due to the biocompatibility, water solubility, and easy to be modified.[30,31] The biofunctional network, which was cross-linked via Michael addition between acrylates groups along the oxidized acrylated hyaluronic acid (OAHA) backbone and the dithiol of matrix metalloproteinase (MMP)-sensitive cross-linkers, is denoted in the document as OAHA-MMP hydrogel (Figure S1a, Supporting Information). The MMP-sensitive peptide cross-linkers are enzymatically degradable peptide units that are susceptible to MMPs secreted by cells.[32,33] In addition, the cell-adhesive RGD peptides were also functionalized on the OAHA chains using a Michael reaction. Both the RGD adhesive peptide and the MMP-sensitive cross-linker add biofunctionality to the OAHA-MMP hydrogels.[34–37] To achieve a self-healing network, the aldehyde groups along the OAHA chains enable secondary cross-linking with the *N*-carboxyethyl chitosan (CEC). This hydrogel is denoted as CEC-OAHA hydrogel. The resultant reversible imine bonds formed from the Schiff base reaction of the amino groups on CEC and the aldehyde groups on OAHA (Figure S1b, Supporting Information), which can establish an intrinsic dynamic equilibrium between bond association and dissociation in the polymer networks, provide the self-healing capability to the hydrogels.[26,28,29] The dual cross-linked CEC-OAHA-MMP hydrogels possess both biofunctionality and self-healing properties under physiological conditions. In addition, the amount of RGD adhesive peptides and MMP-sensitive cross-linkers in the hydrogel networks can be gradually varied as two gradient cues to assess their effects on the encapsulated cell morphology and growth. Green fluorescent protein (GFP)-positive murine sarcoma KrasG12D/+; Ink4a/Arf fl/fl (KIA) tumor cells were encapsulated in the gradient CEC-OAHA-MMP hydrogel to test their responses to gradients of the RGD and MMP peptides.[38] This new biofunctional injectable self-healing hydrogel provides unprecedented opportunities to create modular gradient hydrogel constructs with arbitrary gradient shapes and distributions.

To fabricate the RGD-modified dual cross-linked CEC-OAHA-MMP hydrogel, the OAHA polymer and RGD were dissolved in triethanolamine-buffered saline (TEOA buffer, pH 8.0) and left them to react for 1 h under gentle shaking. Thereafter, the TEOA buffer solution of CEC and MMP was mixed with the OAHA-RGD solution at 37 °C for cross-linking. The solution was mixed uniformly by vortexing, and homogeneous hydrogels were eventually obtained. The TEOA buffer was selected as the solvent because the Michael reaction can be accelerated at pH 8.0, which is near physiological conditions while maintaining cytocompatibility.[32,39–41] The final concentrations of OAHA and CEC were fixed as 4 and 0.4 wt%, respectively, for all samples, to achieve an approximate equivalent molar ratio of reactive groups between CEC and OAHA. While the final concentrations of RGD were

altered from low (0×10^{-3} M) to high (5×10^{-3} M) to low (0.5×10^{-3} M) in intervals of 1×10^{-3} M. The concentrations of the MMP-sensitive cross-linker were altered from low (2.5×10^{-3} M) to high (13×10^{-3} M) to low (3×10^{-3} M) in intervals of 1.5×10^{-3} M to cause them to act as gradients within the CEC-OAHA-MMP networks.

To first study the different physico-chemical properties of the biofunctional and self-healing networks in the newly developed CEC-OAHA-MMP hydrogel, we also synthesized RGD-modified OAHA-MMP (MMP concentration: 5.5×10^{-3} M), CEC-OAHA and CEC-OAHA-MMP (MMP concentration: 5.5×10^{-3} M) hydrogels at a fixed RGD concentration of 3.5×10^{-3} M. The vial inversion method was used to determine the gelation times of the OAHA-MMP, CEC-OAHA, and CEC-OAHA-MMP hydrogels (Figure 1b). The gelation time for the mixed precursor solutions of the three hydrogel samples significantly decreased with mixing time at 37 °C. The OAHA-MMP hydrogel was formed via Michael addition and required the longest time of 12 min. The CEC-OAHA hydrogel was formed from a dynamic Schiff base reaction, which only required 2 min for gelation. The CEC-OAHA-MMP hydrogel was formed within 0.6 min, indicating the collective effect of dual cross-links on the formation kinetics of CEC-OAHA-MMP networks. To test the viscoelastic modulus, we performed rheological measurements of each hydrogel (Figure 1c). The storage moduli (G') of the CEC-OAHA-MMP hydrogel is 775 ± 90 Pa, which is almost twice the sum of the G' of the OAHA-MMP (111 ± 26 Pa) and CEC-OAHA (325 ± 38 Pa) hydrogels. These results indicate that the dual cross-links in the CEC-OAHA-MMP networks intertwined and mutually supported each other instead of simply superimposing, contributing to a significant increase in the storage modulus.

In addition, the reversible imine bonds between CEC and OAHA are self-degradable through hydrolysis due to the water byproduct of the dynamic Schiff base reaction (Figure S1b, Supporting Information). The degradation behaviors of the OAHA-MMP, CEC-OAHA, and CEC-OAHA-MMP hydrogels were investigated by immersing them in KIA-GFP cell culture media (Figure S2, Supporting Information). The CEC-OAHA hydrogel first swelled in the media and fully degraded within 2 d. The CEC-OAHA-MMP hydrogel exhibited continuously increasing weight loss for 6 d compared with the OAHA-MMP hydrogel. In addition to hydrolysis, polypeptides contained in the culture medium (such as growth factors and serum with amino groups) may also contribute to the degradation of the imine bonds in the networks.[28,29] To test the cleavage of the MMP-sensitive cross-links, we encapsulated KIA-GFP cells, which are known to produce MMPs,[38,40] in the CEC-OAHA-MMP hydrogel before immersing in the culture media. As expected, the KIA-GFP-loaded CEC-OAHA-MMP hydrogel was fully degraded within 5 d.

To assess the self-healing performance of the CEC-OAHA-MMP hydrogel and test its potential to generate modular gradient hydrogels, we prepared a series of CEC-OAHA-MMP hydrogel modules stained with a gradient of shades of a blue dye (Figure 1di). Subsequently, a total of eight pieces of the hydrogel modules were combined into an integral hydrogel stripe with a gradient distribution from light to dark blue (Figure 1dii). After 20 min at 37 °C without any external intervention, the boundaries between each of the gradient modules became obscure (Figure 1diii), and the entire hydrogel stripe could be lifted up and deformed under its own weight (Figure 1div–vi). No splitting was observed, demonstrating

that the interphase layer was strong enough to sustain its own weight. To further confirm the healing phenomenon on the microscale, we examined the tightly jointed slit of the two CEC-OAHA-MMP hydrogel modules under a light microscope, and we documented the closure process of the slit at intervals of 3 min. The slit almost disappeared after 21 min, demonstrating the excellent self-healing behavior of the CEC-OAHA-MMP hydrogel. Moreover, the OAHA-MMP hydrogel failed to self-heal due to the lack of dynamic imine cross-links, which are found in the CEC-OAHA and CEC-OAHA-MMP networks (Figure S3, Supporting Information). This demonstrates that dynamic bonds are crucial for the self-healing property of the hydrogel.

Unlike traditional injectable hydrogels, self-healing hydrogels have flowability capability to be injected after gelation.[42–44] The broken hydrogel pieces loaded and squeezed from the syringe can self-assemble and self-heal into an integral hydrogel constructs after removal of the shear force. To prove the flowability of our CEC-OAHA-MMP hydrogel, we first performed continuous step-strain measurements to test its rheological recovery behavior (Figure 2a). Briefly, oscillatory shear strains of 0.1% and 800% were alternately loaded on a disc-shaped CEC-OAHA-MMP hydrogel at a fixed frequency of 1.0 rad s^{-1} at 37 °C, and each strain was maintained for 200 s. At 0.1% strain, G' was larger than the loss modulus (G''), indicating a solid-like CEC-OAHA-MMP hydrogel. However, the G' and G'' values were inverted at 800% strain, indicating that the hydrogels were fully converted into a fluid-like state. Subsequently, after removing the large amplitude oscillatory shear, G' and G'' of the CEC-OAHA-MMP hydrogel recovered to their original values after 90 s of self-healing. This result demonstrates that the CEC-OAHA-MMP hydrogel possesses shear-flowing and standing-gelling properties,[45,46] which can induce quick recovery of the internal networks after a large amplitude oscillatory shear breakdown.

To demonstrate retention of the gradient following injection, we synthesized a series of tiny CEC-OAHA-MMP hydrogel discs (6 mm diameter) with gradients of shades of a blue dye (Figure 2b,c), which were then loaded into a 10 mL syringe in the order of the user-defined gradient distributions (Figure 2d). The loaded hydrogel discs could be sequentially injected on a glass slide from needles with diameters of 0.7 mm (Figure 2ei) and 1.4 mm (Figure 2eii). We could also freely control the gradient distributions of the injected CEC-OAHA-MMP hydrogels by changing the loading sequence of the tiny hydrogel discs (Figure 2eiii) and achieve flexible shapes of the injected hydrogel (Figure 2eiv). These tests demonstrate that the custom-defined gradient distribution and various construct shapes can be facilely generated by the injected manner of CEC-OAHA-MMP hydrogel.

To further evaluate the use of the CEC-OAHA-MMP hydrogel for studying cellular responses to gradients, KIA-GFP cells were encapsulated in the CEC-OAHA-MMP hydrogels with various concentrations of RGD or MMP cross-linker. Tiny disc-shaped units of KIA-GFP-loaded CEC-OAHA-MMP hydrogels were generated and loaded into a syringe in a user-defined distribution of low to high to low (Figure 3ai) and were then injected onto a glass slide equipped with 2 mm thick polydimethylsiloxane (PDMS) pads at each end, to generate stripe-shaped hydrogel construct (Figure 3aii,iii). The slide was covered with a coverslip to achieve uniform thickness of the construct for imaging. After placing in a cell culture incubator for 20 min, KIA-GFP culture media was added to both sides of the fully

self-healed gradient CEC-OAHA-MMP hydrogel construct and continuously cultured for 3 d (Figure S4, Supporting Information).

To examine the effects of the cell-adhesive RGD gradients on KIA-GFP cells, we fabricated RGD gradient CEC-OAHA-MMP hydrogel construct made of 11 tiny units (each is 10 μL) with varying RGD concentrations at an interval of 1×10^{-3} M. The gradient construct was constructed from low (0×10^{-3} M) to high (5×10^{-3} M) to low (0.5×10^{-3} M) concentration (Figure S5a, Supporting Information) with a fixed MMP-sensitive cross-linker concentration of 5.5×10^{-3} M. The KIA-GFP cells were encapsulated into every unit of the CEC-OAHA-MMP hydrogel construct. Fluorescent confocal microscopy images of the entire injected KIA-GFP loaded CEC-OAHA-MMP hydrogel stripe are shown in Figure 3b,c with or without the hydrogel background. The encapsulated KIA-GFP cells tolerated the 3D environment of the gradient CEC-OAHA-MMP hydrogel construct. Elongation of the encapsulated KIA-GFP cells was observed in the high RGD section of the hydrogel and was compared with the low RGD section on both sides, as documented using 3D and z-axis maximum projection views of the confocal images (Figure 3dii,ii′). The average aspect ratio of the encapsulated KIA-GFP cells in the high RGD section was significantly higher than that of the KIA-GFP cells in the lower RGD section (Figure 3d), indicating that the high RGD concentration regulates KIA-GFP elongation.

We next assessed the effect of the MMP-sensitive cross-linker gradients on the KIA-GFP cells. Here, we used 15 units (each is 10 μL) with varying concentrations of a proteolytic-degraded peptide of MMP-sensitive cross-linker, at an interval of 1.5×10^{-3} M. The gradient construct was fabricated from low (2.5×10^{-3} M) to high (13×10^{-3} M) to low (3×10^{-3} M) concentration (Figure S5b, Supporting Information) with a fixed RGD concentration of 3.5×10^{-3} M. The KIA-GFP cells were encapsulated into every unit of the CEC-OAHA-MMP hydrogel. Fluorescent confocal microscopy images of the whole injected KIA-GFP-loaded CEC-OAHA-MMP hydrogel construct are shown in Figure 3a,b. The encapsulated KIA-GFP cells tolerated the 3D environment of the gradient CEC-OAHA-MMP hydrogel. More elongation of the encapsulated KIA-GFP cells was observed in the high MMP-sensitive cross-linker section of the hydrogel (Figure 4dii,ii′) using the 3D and z-axis maximum projection views of the confocal images. The average aspect ratios of the encapsulated KIA-GFP cells significantly increased with increasing MMP-sensitive cross-linker contents (Figure 4d), illustrating that higher proteolytic-degraded peptide content in the hydrogel enables KIA-GFP cell elongation in the 3D construct. Collectively, these results establish that our newly developed injectable and self-healing CEC-OAHA-MMP hydrogel can be utilized to generate smart modular gradient hydrogel constructs in which the encapsulated cells can effectively respond to gradient cues.

In summary, we report a novel modular gradient hydrogel construct with controllable gradient distributions and flexible shapes by developing a dual cross-linked biofunctional and self-healing CEC-OAHA-MMP hydrogel. The resultant dynamic imine bonds formed in the dual-cross-linked networks enable the self-healing capability of the hydrogel under physiological conditions. The encapsulated KIA-GFP cells were found to be responsive to the gradient concentrations of RGD peptides and MMP-sensitive cross-linkers in the CEC-OAHA-MMP hydrogel. This approach offers opportunities to use self-healing hydrogels

to generate modular gradient hydrogel constructs. With further refinement, our technique can be expanded to working with patient-specific cells or stem cells, combining multiple chemical or physical gradient cues and screening cellular responses by tracking cell proliferation, migration, or differentiation tendencies in the modular gradient hydrogel system. Moreover, by exploiting the injectable and self-healing characteristics of the CEC-OAHA-MMP hydrogels, we may be able to build cell coculture systems and recreate the complex environments of native tissues, ultimately using such hydrogels for tissue regeneration.

Experimental Section

Materials:

Chitosan (degree of deacetylation, 77%, MW: 50–190 kDa), acrylic acid, sodium periodate, dimethylaminopyridine, and triethanolamine-buffered saline were purchased from Sigma-Aldrich. Hyaluronic acid (MW: 90 kDa) was obtained from LifeCore Biomedical in Chaska, MN. The cell-adhesive peptide GCGYGRGDSPG (RGD, MW: 1025.06 Da, greater than 95% purity) and MMP-sensitive peptide cross-linker GCRDGPQGWGQDRCG (MMP, MW: 1704.85 Da, greater than 95% purity) were purchased from Genscript. All other chemicals were analytical grade and used without further purification.

Synthesis of CEC:

CEC was prepared via a previous method using Michael's reaction.[28] Briefly, chitosan (1.0 g, 6.2 mmol) was dissolved in 50 mL distilled water containing acrylic acid (1.46 mL, 21.3 mmol), and the mixture was magnetically stirred at 50 °C for 3 d. Then, the pH of the solution was adjusted to 10–12 using 1 mol L^{-1} NaOH. Thereafter, the solution was dialyzed (MWCO 8000) against distilled water for 3 d with the water repeatedly changed, followed by freeze-drying to obtain pure CEC powder. ^{1}H NMR (400 MHz, D_2O, δ): 1.94 (s, 3H, $COCH_3$), 2.83 (s, 2H, CH_2CO_2Na), 3.30–4.87 (m, glucosamine). The degree of substitution was 29%, which was determined in the ^{1}H NMR spectra by comparing the peak area of the acetamide methyl protons ($\delta = 1.94$) in the chitosan and the methylene protons ($\delta = 2.83$) in acrylic acid in CEC.

Synthesis of the Tetrabutylammonium Salt of Hyaluronic Acid (HA-TBA):

HA-TBA was synthesized as reported previously.[33] HA (1.0 g, 2.5 mmol) was dissolved in 200 mL water to achieve a 1 wt% solution. The highly acidic ion exchange resin, Dowex-100 (3.0 g), was then added to the HA solution. After stirring for 8 h, the solution was filtered to remove the resin and then neutralized with 0.2 M tetrabutylammonium hydroxide (TBA-OH) to a pH of ≈7. The HA-TBA was obtained after lyophilization. ^{1}H NMR (400 MHz, D_2O, δ): 4.2–4.6 (d, 2H), 3.2–4.0 (10H), 3.0 (dd, 8H), 2.0 (s, 3H), 1.5 (8H), 0.8 (12H).

Synthesis of Acrylated Hyaluronic Acid (AHA):

AHA was also synthesized as reported previously[32,33] Briefly, HA-TBA (1 g, 1.6 mmol) and acrylic acid (0.33 mL, 4.8 mmol) were combined in the presence of dimethylaminopyridine (0.03 g, 0.24 mmol) and di-*tert*-butyl dicarbonate (1.05 g, 4.8 mmol)

in 200 mL DMSO. Thereafter, the solution was dialyzed (MWCO 8000) against distilled water for 3 d with the water repeatedly changed, followed by freeze-drying to obtain the pure AHA. ^{1}H NMR (400 MHz, D_2O, δ): 5.9–6.4 (3H), 4.2–4.6 (d, 2H), 3.2–4.0 (10H), 3.0 (dd, 8H), 2.0 (s, 3H). HA that had 32% of its hydroxy groups acrylate-modified was measured using ^{1}H NMR.

Synthesis of OAHA:

The synthesis of OAHA was based on a reported method with a slight modification[47,48] AHA (1.0 g, 2.4 mmol) was dissolved in 50 mL distilled water. Then, sodium periodate (1.08 g, 0.5 mmol) was added, and the solution was magnetically stirred in the dark for 1.5 h. The reaction was terminated by adding ethylene glycol (0.5 mL) and stirring for an additional 1 h. After the reaction, the mixture was dialyzed (MWCO 8000) against distilled water for 3 d with the water repeatedly changed, followed by lyophilization to obtain OAHA. The oxidation percentage of OAHA was 11%, which was quantified by measuring the number of aldehydes in the polymer using *t*-butyl carbazate.[49]

Preparation of the CEC-OAHA-MMP Hydrogel:

For hydrogel formation, the OAHA polymer and the cell-adhesive peptides (RGD) were dissolved in TEOA buffer (pH 8.0) and left to react for 1 h under gentle shaking. Thereafter, the TEOA buffer solution of CEC and MMP was mixed with the OAHA-RGD solution at 37 °C for cross-linking. The solution was mixed uniformly by vortexing, and homogeneous hydrogels were eventually obtained. The final concentrations of OAHA and CEC were fixed as 4 and 0.4 wt%, respectively, while the final concentrations of RGD were altered from low (0×10^{-3} M) to high (5×10^{-3} M) to low (0.5×10^{-3} M) in intervals of 1×10^{-3} M. The concentrations of the MMP-sensitive cross-linker were altered from low (2.5×10^{-3} M) to high (13×10^{-3} M) to low (3×10^{-3} M) in intervals of 1.5×10^{-3} M to cause them to act as gradients within the CEC-OAHA-MMP networks. The CEC-OAHA (CEC concentration: 0.4 wt%) and OAHA-MMP hydrogels (MMP concentration: 5.5×10^{-3} M) were also synthesized by maintaining the final OAHA concentration at 4 wt% and RGD concentration at 3.5×10^{-3} M.

Measurement of Gelation Time:

The gelation time of the CEC-OAHA, OAHA-MMP, and CEC-OAHA-MMP hydrogels was determined using the vial inversion method[16,29] The precursor solutions of the hydrogel were mixed gently to initiate the cross-linking reaction at 37 °C. The gelation time was measured as the time point after inverting the solution when more than 3 min passed without flow. All the gelling times were measured in triplicate for each group.

Measurement of the Degradation Ratio:

The degradation of the CEC-OAHA, OAHA-MMP, CEC-OAHA-MMP, and KIA-GFP-loaded CEC-OAHA-MMP hydrogels (cell density: 3 million mL^{-1}) with a fixed MMP concentration of 5.5×10^{-3} M and a fixed RGD concentration of 3.5×10^{-3} M were determined by weighing the samples at different times. The hydrogels (W_0) were immersed in microtubes with 500 μL KIA-GFP culture medium at 37 °C. The medium was removed

from each sample at predetermined times. The weight of each sample (W_t) was measured. Fresh medium was added to the microtubes after each weighing. The degradation ratio was calculated by (W_t/W_0) × 100%.

Rheological Measurements:

(1) The storage moduli (G') of the CEC-OAHA, OAHA-MMP, and CEC-OAHA-MMP hydrogel discs (8 mm in diameter) with fixed MMP and RGD concentrations of 5.5×10^{-3} and 3.5×10^{-3} M, respectively, were tested using a rheometer equipped with an 8 mm parallel plate at 37 °C. Under a fixed strain of 0.1%, the angular frequency was swept from 0.1 to 100 rad s^{-1}. (2) The alternate step strain sweep of the CEC-OAHA-MMP hydrogel discs was measured at a fixed angular frequency (10 rad s^{-1}) at 37 °C. Amplitude oscillatory strains were switched from a small strain (γ = 0.1%) to a subsequent large strain (γ = 800%) and back to a small strain (γ = 0.1%) after waiting for 90 s of healing time. Each strain was induced for 200 s.

Self-Healing Experiments:

(1) Four separated parts of the disc-shaped OAHA-MMP, CEC-OAHA, and CEC-OAHA-MMP hydrogels were prepared, and two were stained with blue dye. Then, they were alternatively combined into blended integral hydrogel discs and kept for 20 min without any external intervention at 37 °C. Then, their self-healing ability was checked by observing the contacted boundaries and lifting the hydrogels using tweezers. (2) The eight pieces of tiny cubic CEC-OAHA-MMP hydrogel modules (6 mm × 6 mm) stained with the gradient blue dye were synthesized in a PDMS mold. Then, the modules were combined together and placed in a 37 °C incubator for 20 min before checking the integrity of the hydrogels. (3) The jointed slit between two CEC-OAHA-MMP hydrogel modules was observed every 3 min using a light microscopy to check for disappearance of the slit.

Injection of the CEC-OAHA-MMP Modular Gradient Hydrogel:

Mixed precursor solutions of OAHA (4 wt%), RGD (3.5×10^{-3} M), CEC (0.4 wt%), and the MMP-sensitive cross-linker (5.5×10^{-3} M) with gradient blue dye were placed into a circular PDMS mold. A series of tiny CEC-OAHA-MMP hydrogel discs (6 mm diameter) with gradient blue dye were formed and loaded into a 10 mL syringe in the designed sequence. The hydrogel discs were injected on a glass slide using different needle diameters (0.7 and 1.4 mm). They can also be injected with different gradient distributions and unlimited shapes.

Encapsulation of KIA-GFP Cells in CEC-OAHA-MMP Modular Gradient Hydrogel:

(1) To evaluate the cell response to the CEC-OAHA-MMP hydrogel with the RGD gradient, KIA-GFP cells were loaded in each CEC-OAHA-MMP hydrogel unit at a density of 3 million mL^{-1}. Briefly, mixed solutions of OAHA (4 wt%), CEC (0.4 wt%), the MMP-sensitive cross-linker (5.5×10^{-3} M) with 11 gradients of different RGD concentrations from low (0×10^{-3} M) to high (5×10^{-3} M) to low (0.5×10^{-3} M) at intervals of 1×10^{-3} M were separately mixed with centrifuged KIA-GFP cells. The 10 μL mixture with the suspended cells of each RGD concentration was placed into a PDMS circular mold.

After gelation, the 11 pieces of KIA-GFP-loaded RGD modular gradient hydrogels were sequentially loaded into a 10 mL syringe and injected on a glass slide that was equipped with 2 mm thick PDMS. A coverslip was placed over the injected modular gradient hydrogel to obtain a 2 mm thick hydrogel stripe. The hydrogel stripe was placed in a 37 °C incubator for 20 min, after which KIA-GFP culture media was added to fully cover the self-healed hydrogel stripe. The constructs were then continuously cultured for 3 d with daily media change, before observation by confocal microscopy. The aspect ratio of the elongated encapsulated KIA-GFP cells was analyzed using a custom MATLAB script. Confocal images from three different RGD gradient sections were analyzed by randomly selecting ten views of each section. (2) For the cellular response tests of the CEC-OAHA-MMP hydrogel with MMP-sensitive cross-linker gradient, KIA-GFP cells were loaded in each CEC-OAHA-MMP hydrogel unit at a density of 3 million mL^{-1}. Briefly, mixed solutions of OAHA (4 wt%), CEC (0.4 wt%), and RGD (3.5×10^{-3} M) with 15 gradients of different MMP-sensitive cross-linker concentrations from low (2.5×10^{-3} M) to high (13×10^{-3} M) to low (3.0×10^{-3} M) at intervals of 1.5×10^{-3} M were separately mixed with centrifuged KIA-GFP cells. The 10 μL mixtures of suspended cells of each MMP-sensitive cross-linker concentration were placed into a PDMS circular mold. After gelation, the 15 pieces of KIA-GFP-loaded MMP-sensitive cross-linker modular gradient hydrogels were sequentially loaded into a 10 mL syringe and then injected onto a glass slide equipped with 2 mm thick PDMS. A coverslip was placed over the injected modular gradient hydrogel to obtain a 2 mm thick hydrogel stripe. The hydrogel stripe was placed in a 37 °C incubator for 20 min, after which KIA-GFP culture media was added to fully cover the self-healed hydrogel stripe. The constructs were then continuously cultured for 3 d with daily media change, before observation by confocal microscopy. The aspect ratio of the elongated encapsulated KIA-GFP cells was analyzed using a custom MATLAB script. Confocal images from three different RGD gradient sections were analyzed by randomly selecting ten views of each section.

Supplementary Material

Refer to Web version on PubMed Central for supplementary material.

Acknowledgements

The authors would like to thank T. S. Eisinger (UPenn) for generously providing the KIA-GFP cells. This work was supported by fellowship from Nanotechnology Cancer Research training grant (2T32CA153952-06, to D.M.L.), and the American Heart Association (15EIA22530000), The NCI Physical Sciences-Oncology Center (U54CA210173), and the President's Frontier Award from Johns Hopkins University (all to S.G.).

References

[1]. Hickson SS, Nichols WW, McDonnell BJ, Cockcroft JR, Wilkinson IB, McEniery CM, Hypertens. Res 2016, 39, 723. [PubMed: 27334244]

[2]. Oh SH, An DB, Kim TH, Lee JH, Acta Biomater 2016, 35, 23. [PubMed: 26883774]

[3]. Truong AS, Lockett MR, Analyst 2016, 141, 3874. [PubMed: 27138213]

[4]. Joyal J-S, Sun Y, Gantner ML, Shao Z, Evans LP, Saba N, Fredrick T, Burnim S, Kim JS, Patel G, Nat. Med 2016, 22, 692.

[5]. Sylow L, Kleinert M, Richter EA, Jensen TE, Nat. Rev. Endocrinol 2017. 13, 133. [PubMed: 27739515]

[6]. Lutolf MP, Gilbert PM, Blau HM, Nature 2009, 462, 433. [PubMed: 19940913]

[7]. Rana D, Kumar TS, Ramalingam M, J. Biomater. Tissue Eng 2014, 4, 507.

[8]. Sant S, Hancock MJ, Donnelly JP, Iyer D, Khademhosseini A, Can. J. Chem. Eng 2010, 88, 899. [PubMed: 21874065]

[9]. Tingting X, Wanqian L, Li Y, J. Biomed. Mater. Res., Part A, 2017, 105, 1799.

[10]. Brandenberg N, Lutolf MP, Adv. Mater 2016, 28, 7450. [PubMed: 27334545]

[11]. Somaweera H, Ibraguimov A, Pappas D, Anal. Chim. Acta 2016, 907, 7. [PubMed: 26802998]

[12]. Eltaher HM, Yang J, Shakesheff KM, Dixon JE, Acta Biomater 2016, 41, 181. [PubMed: 27265151]

[13]. Wang L, Li Y, Huang G, Zhang X, Pingguan-Murphy B, Gao B, Lu TJ, Xu F, Crit. Rev. Biotechnol 2016, 36, 553. [PubMed: 25641330]

[14]. Pampaloni F, Reynaud EG, Stelzer EH, Nat. Rev. Mol. Cell Biol 2007, 8, 839. [PubMed: 17684528]

[15]. Tibbitt MW, Anseth KS, Biotechnol. Bioeng 2009, 103, 655. [PubMed: 19472329]

[16]. Park KM, Gerecht S, Nat. Commun 2014, 5, 4075. [PubMed: 24909742]

[17]. Kusuma S, Shen Y-I, Hanjaya-Putra D, Mali P, Cheng L, Gerecht S, Proc. Natl. Acad. Sci. USA 2013, 110, 12601. [PubMed: 23858432]

[18]. Sun G, Zhang X, Shen Y-I, Sebastian R, Dickinson LE, Fox-Talbot K, Reinblatt M, Steenbergen C, Harmon JW, Gerecht S, Proc. Natl. Acad. Sci. USA 2011, 108, 20976. [PubMed: 22171002]

[19]. Park KM, Gerecht S, Eur. Polym. J 2015, 72, 507.

[20]. Norris SC, Tseng P, Kasko AM, ACS Biomater. Sci. Eng 2016, 2, 1309. [PubMed: 33434984]

[21]. Odedra D, Chiu LL, Shoichet M, Radisic M, Acta Biomater 2011, 7, 3027. [PubMed: 21601017]

[22]. Guarnieri D, De Capua A, Ventre M, Borzacchiello A, Pedone C, Marasco D, Ruvo M, Netti P, Acta Biomater 2010, 6, 2532. [PubMed: 20051270]

[23]. Du Y, Hancock MJ, He J, Villa-Uribe JL, Wang B, Cropek DM, Khademhosseini A, Biomaterials 2010, 31, 2686 [PubMed: 20035990]

[24]. He J, Du Y, Villa-Uribe JL, Hwang C, Li D, Khademhosseini A, Adv. Funct. Mater 2010, 20, 131. [PubMed: 20216924]

[25]. Wong JY, Velasco A, Rajagopalan P, Pham Q, Langmuir 2003, 19, 1908.

[26]. Wei Z, Yang JH, Zhou J, Xu F, Zrínyi M, Dussault PH, Osada Y, Chen YM, Chem. Soc. Rev 2014, 43, 8114. [PubMed: 25144925]

[27]. Wei Z, Yang JH, Du XJ, Xu F, Zrinyi M, Osada Y, Li F, Chen YM, Macromol. Rapid Commun 2013, 34, 1464. [PubMed: 23929621]

[28]. Wei Z, Yang JH, Liu ZQ, Xu F, Zhou JX, Zrínyi M, Osada Y, Chen YM, Adv. Funct. Mater 2015, 25, 1352.

[29]. Wei Z, Zhao J, Chen YM, Zhang P, Zhang Q, Sci. Rep 2016, 6, 37841. [PubMed: 27897217]

[30]. Tharanathan RN, Kittur FS, Crit. Rev. Food Sci. Nutr 2003, 43, 61. [PubMed: 12587986]

[31]. Burdick JA, Prestwich GD, Adv. Mater 2011, 23, 41.

[32]. Hanjaya-Putra D, Bose V, Shen Y-I, Yee J, Khetan S, Fox-Talbot K, Steenbergen C, Burdick JA, Gerecht S, Blood 2011, 118, 804. [PubMed: 21527523]

[33]. Khetan S, Katz JS, Burdick JA, Soft Matter 2009, 5, 1601.

[34]. Bayless KJ, Salazar R, Davis GE, Am. J. Pathol 2000, 156, 1673. [PubMed: 10793078]

[35]. Cuchiara MP, Gould DJ, McHale MK, Dickinson ME, West JL, Adv. Funct. Mater 2012, 22, 4511. [PubMed: 23536744]

[36]. Khetan S, Guvendiren M, Legant WR, Cohen DM, Chen CS, Burdick JA, Nat. Mater 2013, 12, 458. [PubMed: 23524375]

[37]. DeForest CA, Polizzotti BD, Anseth KS, Nat. Mater 2009, 8, 659. [PubMed: 19543279]

[38]. Lewis DM, Park KM, Tang V, Xu Y, Pak K, Eisinger-Mathason TK, Simon MC, Gerecht S, Proc. Natl. Acad. Sci. USA 2016, 113, 9292. [PubMed: 27486245]

[39]. Gjorevski N, Sachs N, Manfrin A, Giger S, Bragina ME, Ordóñez-Morán P, Clevers H, Lutolf MP, Nature 2016, 539, 560. [PubMed: 27851739]

[40]. Shen Y-I, Abaci HE, Krupski Y, Weng L-C, Burdick JA, Gerecht S, Biomater. Sci 2014, 2, 655. [PubMed: 24748963]

[41]. Liu ZQ, Wei Z, Zhu XL, Huang GY, Xu F, Yang JH, Osada Y, Zrínyi M, Li JH, Chen YM, Colloids Surf., B 2015, 128, 140.

[42]. Tseng TC, Tao L, Hsieh FY, Wei Y, Chiu IM, Hsu SH, Adv. Mater 2015, 27, 3518. [PubMed: 25953204]

[43]. Lü S, Gao C, Xu X, Bai X, Duan H, Gao N, Feng C, Xiong Y, Liu M, ACS Appl. Mater. Interfaces 2015, 7, 13029. [PubMed: 26016388]

[44]. Yang B, Zhang Y, Zhang X, Tao L, Li S, Wei Y, Polym. Chem 2012, 3, 3235.

[45]. Sano K-I, Kawamura R, Tominaga T, Oda N, Ijiro K, Osada Y, Biomacromolecules 2011, 12, 4173. [PubMed: 22011361]

[46]. Hou X, Gao D, Yan J, Ma Y, Liu K, Fang Y, Langmuir 2011, 27, 12156. [PubMed: 21866964]

[47]. Liu Y, Chan-Park MB, Biomaterials 2009, 30, 196. [PubMed: 18922573]

[48]. Tan H, Chu CR, Payne KA, Marra KG, Biomaterials 2009, 30, 2499. [PubMed: 19167750]

[49]. Bouhadir KH, Hausman DS, Mooney DJ, Polymer 1999, 40, 3575.

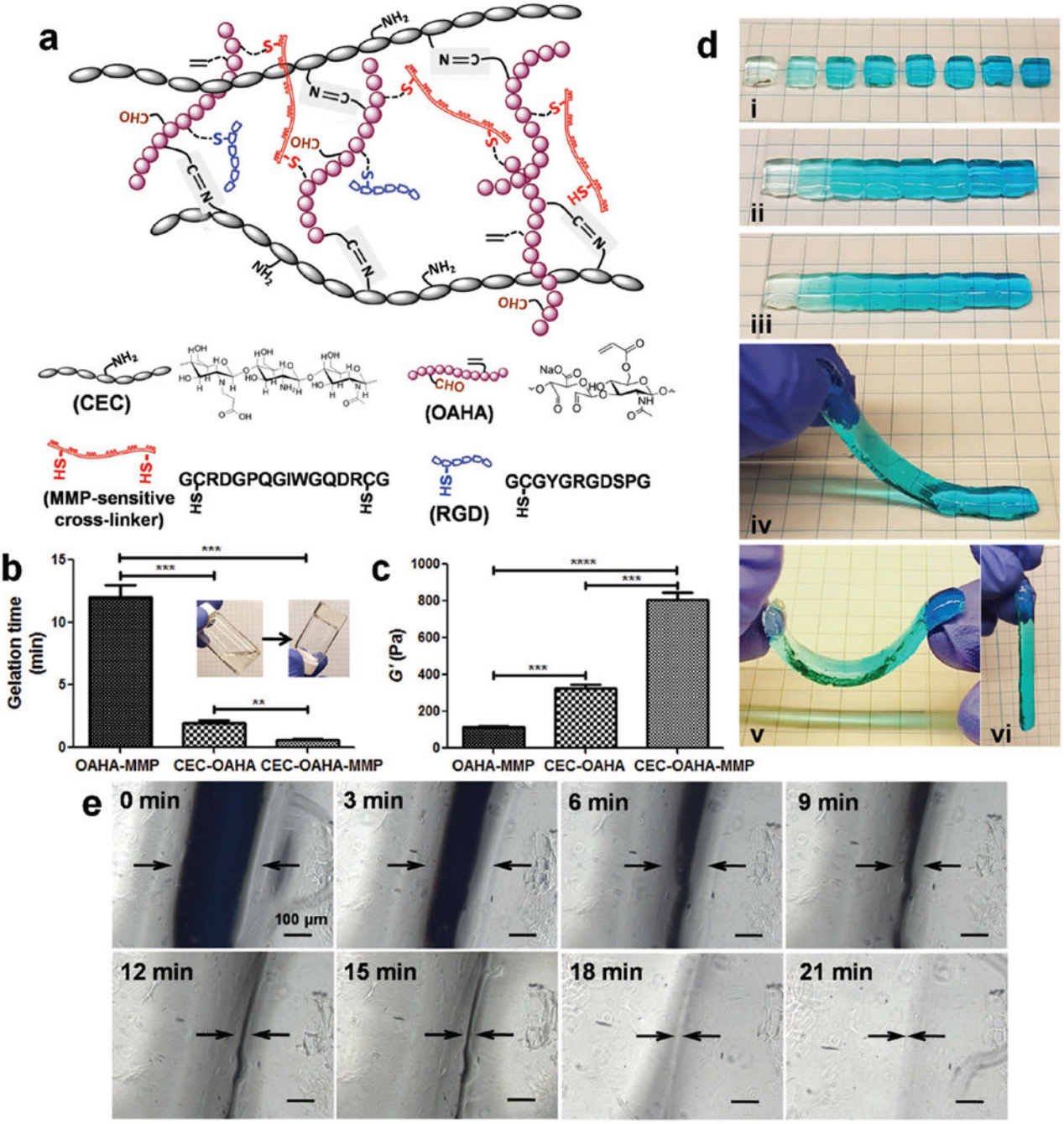

Figure 1.

Structure and self-healing properties of the CEC-OAHA-MMP hydrogels. a) Network and chemical structures of the RGD-immobilized CEC-OAHA-MMP hydrogel. b) Gelation times of the OAHA-MMP, CEC-OAHA, and CEC-OAHA-MMP hydrogels. c) Storage moduli (G') of the OAHA-MMP, CEC-OAHA, and CEC-OAHA-MMP hydrogels. Error bars represent standard deviations ($n = 3$). Significance levels were set at $^{**}P < 0.01$, $^{***}P < 0.001$, and $^{****}P < 0.0001$. d) The CEC-OAHA-MMP hydrogel modules stained with gradient blue dye were synthesized in a PDMS mold (i). After combining the modules

together and maintaining at 37 °C for 20 min (ii), the hydrogels self-healed, as the integrity and boundaries between different hydrogel modules had nearly disappeared (iii). The self-healed hydrogel could also be handled and lifted without fractures (iv–vi). e) Microscopic observations of the tightly jointed slit (indicated by arrows) between two CEC-OAHA-MMP hydrogel modules. The slit was observed every 3 min, which almost disappeared after 21 min. The scale bar is 100 μm.

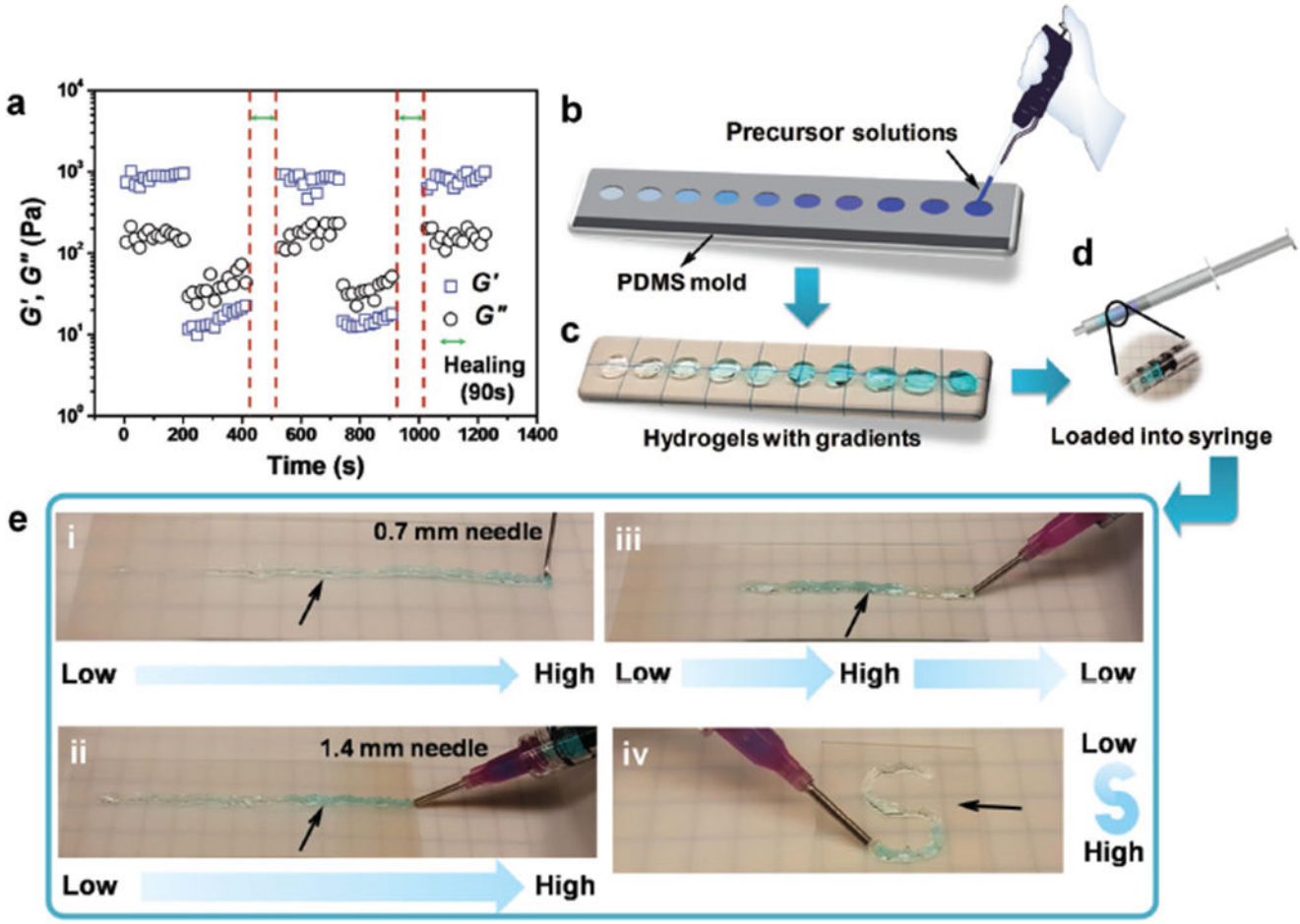

Figure 2.

Rheological recovery test and procedure for generating modular gradient hydrogel construct by injection. a) The G' and G'' of the CEC-I-OSA hydrogel from alternate step-strain sweeps with a small strain (γ = 0.1%) for 200 s, followed by a large strain (γ = 800%) for 200 s after healing for 90 s at 37 °C. b) The mixed precursor solutions of the hydrogels containing various concentration of blue dye were placed into the circular PDMS mold, generating the "units." c,d) The CEC-OAHA-MMP hydrogel units with varying concentration of blue dye were removed from the mold and loaded into a 10 mL syringe. e) The CEC-OAHA-MMP hydrogel units were sequentially injected from needles (indicated by arrows) to generate gradient hydrogel constructs with different needle diameters (0.7 and 1.4 mm), gradient distributions (i, ii, and iii) and "S" shapes (iv).

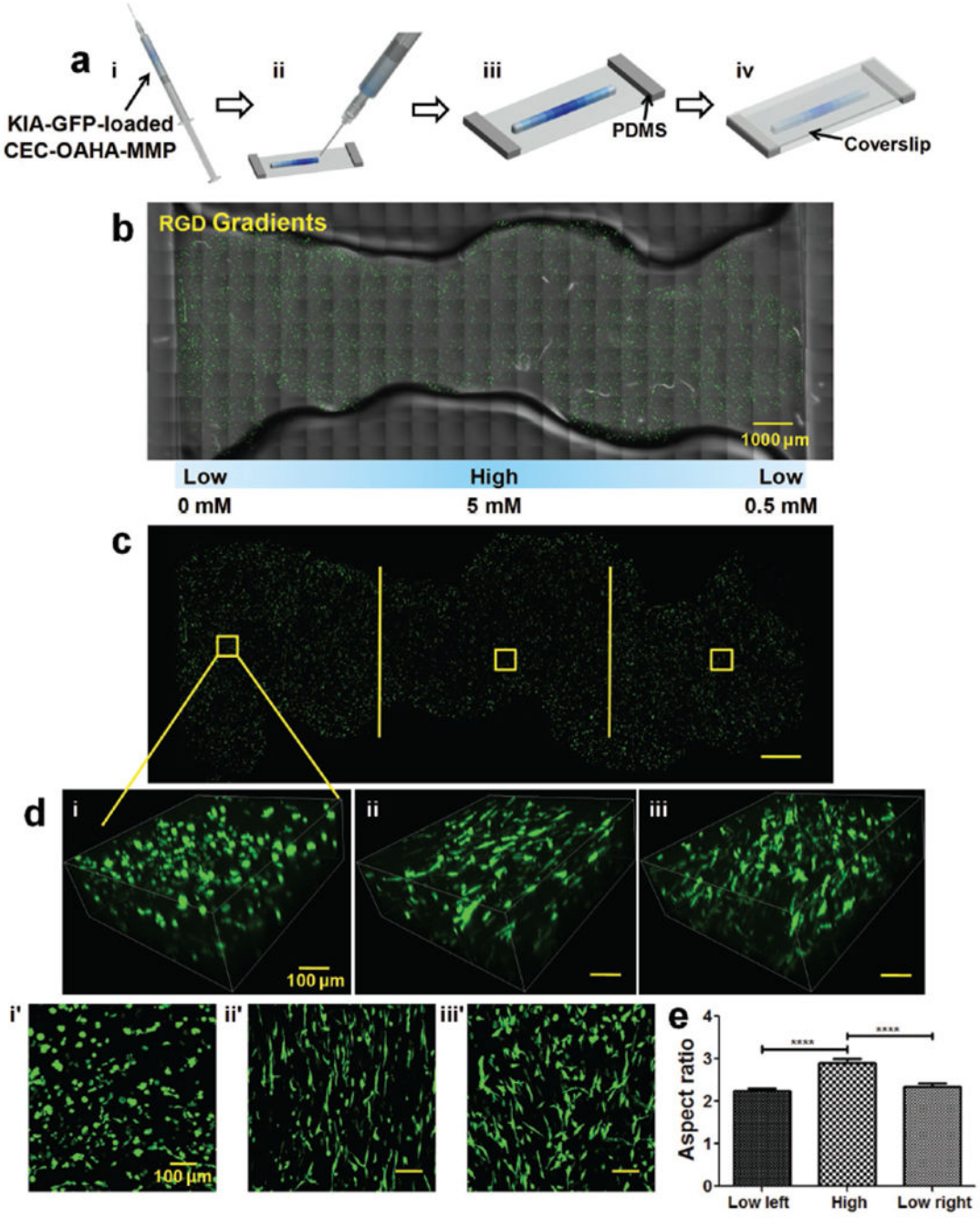

Figure 3.

Generation of cell-loaded gradient hydrogel constructs and cancer cell response to RGD gradients a) Preparation of KIA-GFP-loaded CEC-OAHA-MMP modular gradient hydrogel constructs for microscopic observation. (i) The tiny discs of the CEC-OAHA-MMP hydrogels with various concentrations (here illustrated with blue color) were loaded into the syringe and then injected to generate stripe-shaped construct onto a glass slide equipped with 2 mm thick PDMS (ii and iii). (iv) A coverslip was placed over the injected hydrogel to obtain a 2 mm thick hydrogel stripe. b,c) Confocal images of the entire injected KIA-GFP-

loaded CEC-OAHA-MMP hydrogel stripe-shaped construct with RGD gradient distributions from 0 to 5×10^{-3} to 0.5×10^{-3} M after culturing for 3 d (the encapsulated KIA-GFP cells are green), scale bar: 1000 μm. d) 3D and *z*-axis maximum projection views of confocal images of encapsulated KIA-GFP cell spatial distribution and morphology from the left lower RGD section (i and i′), the high RGD section (ii and ii′), and the right lower RGD section (iii and iii′), scale bar: 100 μm. e) Aspect ratio analysis of the encapsulated KIA-GFP cells from different gradient sections (for each section, we randomly selected ten views for the calculation). Significance levels were set at ****$P < 0.0001$.

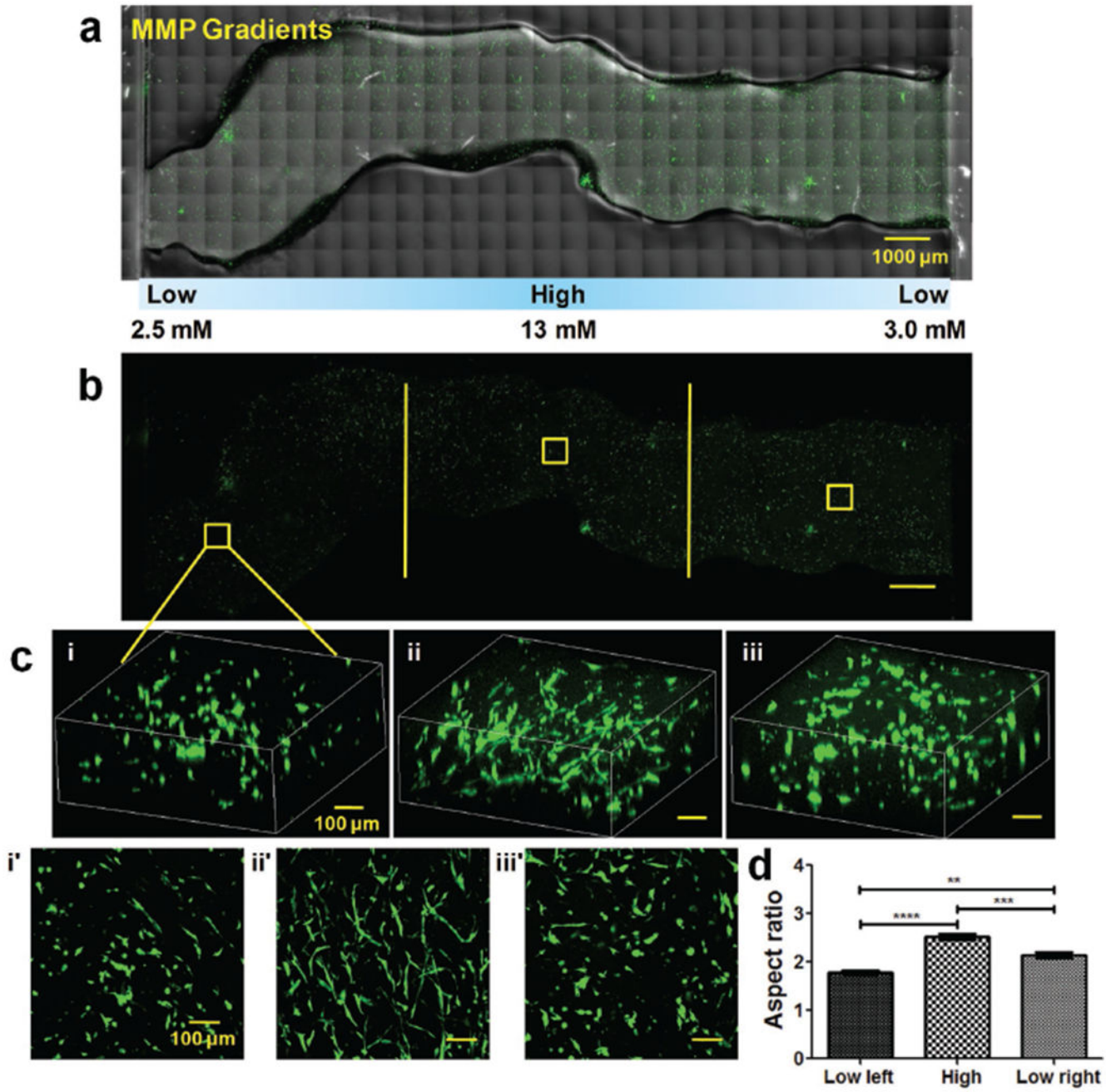

Figure 4.

Cancer cell response to MMP-sensitive cross-linker gradients. a) Confocal images of the entire injected KIA-GFP-loaded CEC-OAHA-MMP hydrogel stripe-shaped construct with MMP-sensitive cross-linker gradient distributions from 2.5×10^{-3} to 13×10^{-3} to 3.0×10^{-3} M after culturing for 3 d (the encapsulated KIA-GFP cells are green), scale bar: 1000 μm. b) Confocal images of the entire view of encapsulated KIA-GFP cells, scale bar: 1000 μm. d) 3D and *z*-axis maximum projection views of the confocal images of the encapsulated KIA-GFP cell spatial distribution and morphology from the left lower MMP-sensitive cross-linker section (i and i′), the high MMP-sensitive cross-linker section (ii and ii′), and the

right lower MMP-sensitive cross-linker section (iii and iii′), scale bar: 100 μm. e) Aspect ratio analysis of the encapsulated KIA-GFP cells from different gradient sections (for each section, we randomly selected ten views for the calculation). Significance levels were set at $^{**}P < 0.01$, $^{***}P < 0.001$, and $^{****}P < 0.0001$.